9. Cody R, Hutchins G, Wahl RL. PET imaging of primary and metastatic breast cancer with 2-fluoro-18F-2-deoxy-d-glucose (FDG) [Abstract]. *Proc Am Soc Clin Oncol* 1990;9:A189.
10. Paul R, Parviainen S. Dynamic [^{18}F]-2-fluoro-2-deoxy-D-glucose (FDG) scintigraphy of normal and tumor-bearing rats. *Res Exp Med (Berl)* 1986;186(4):249–258.
11. Snyder F, Wood R. Alkyl and alk-1-enyl ethers of glycerol in lipids from normal and neoplastic human tissues. *Cancer Res* 1969;29:251–257.
12. Snyder F, Blank ML, Morris HP. Occurrence and nature of O-alkyl and O-alk-1-enyl moieties of glycerol in lipids of Morris transplanted hepatomas and normal rat livers. *Biochim Biophys Acta* 1969;176:502–510.
13. Soodsma JF, Piantadosi C, Snyder F. The biocleavage of alkyl glyceryl ethers in Morris hepatomas and other transplantable neoplasms. *Cancer Res* 1970;30:309–311.
14. Meyer KL, Schwendner SW, Counsell RE. Potential tumor or organ imaging agents 30. Radioiodinated phospholipid ethers. *J Med Chem* 1989;32:2142–2147.
15. Counsell RE, Schwendner SW, Meyer KL, Haradahira T, Gross MD. Tumor visualization with a radioiodinated phospholipid ether. *J Nucl Med* 1990;31:332–336.
16. Plotzke KP, Haradahira T, Stancato L, et al. Selective localization of radioiodinated alkylphosphocholine derivatives in tumors. *Nucl Med Biol* 1992;19:775–782.
17. Plotzke KP, Fisher SJ, Wahl RL, Olken NM, Skinner S, Gross MD, Counsell RE. Selective localization of a radioiodinated phospholipid ether analog in human tumor xenografts. *J Nucl Med* 1993;34:787–792.
18. Ethier SP. Primary culture and serial passage of normal and carcinogen-treated rat mammary epithelial cells in vitro. *J Natl Cancer Inst* 1985;74:1307–1318.
19. Ethier SP, Cundiff KC. Importance of extended growth potential and growth factor independence on in vivo neoplastic potential of primary rat mammary carcinoma cells. *Cancer Res* 1987;47:5316–5322.
20. Ethier SP, Moorthy R. Multiple growth factor independence in rat mammary carcinoma cells. *Breast Cancer Res Treat* 1991;18:73–81.
21. Simpson RU, Arnold AJ. Calcium antagonizes 1,25-dihydroxyvitamin D3 inhibition of breast cancer cell proliferation. *Endocrinology* 1986;119:2284–2289.
22. Simpson RU, Taylor JT. Regulation of cancer cell proliferation by calcium antagonists. *Exper Oncol (Life Sci Adv)* 1988;7:81–89.
23. Taylor JT, Simpson RU. Inhibition of cancer cell growth by calcium channel antagonists in the athymic mouse. *Cancer Res* 1992;52:2413–2418.
24. Weichert JP, VanDort ME, Groziak MP, Counsell RE. Radioiodination via isotope exchange in pivalic acid. *Appl Radiat Isot* 1986;37:907–913.
25. Folch J, Lees M, Sloane-Stanley FG. A simple method for the isolation of total lipids from animal tissues. *J Biol Chem* 1957;226:497–509.
26. Brown RS, Leung JY, Fisher SJ, Frey KA, Ethier SP, Wahl RL. Intratumoral distribution of tritiated fluorodeoxyglucose in breast carcinoma: I. Are inflammatory cells important? *J Nucl Med* 1995;36:1854–1861.
27. Brown RS, Fisher SJ, Wahl RL. Autoradiographic evaluation of the intratumoral distribution of 2-deoxy-D-glucose and monoclonal antibodies in xenografts of human ovarian adenocarcinoma. *J Nucl Med* 1993;34:75–82.
28. Plotzke KP, Rampy MA, Meyer K, et al. Biodistribution, metabolism, and excretion of radioiodinated phospholipid ether analogs in tumor-bearing rats. *J Nucl Biol Med* 1993;37:264–272.

Intraperitoneal Indium-111- and Yttrium-90-Labeled Human IgM (AC6C3-2B12) in Nude Mice Bearing Peritoneal Carcinomatosis

Syed M. Quadri, Atif B. Malik, Hung B. Chu, Ralph S. Freedman and Huibert M. Vriesendorp
Departments of Experimental Radiotherapy and Gynecological Oncology, University of Texas M.D. Anderson Cancer Center, Houston, Texas

Radiolabeled monoclonal antibodies are utilized increasingly for the diagnosis and treatment of human cancer. Tumor targeting of radiolabeled human monoclonal IgM improves with compartmental administration and might be useful for the diagnosis or treatment of peritoneal carcinomatosis. **Methods:** A human monoclonal antibody IgMλ (AC6C3-B12) reactive with human adenocarcinomas was conjugated to isothiocyanato-2-benzyl-3-methyl-diethylenetriamine-penta-acetic acid and labeled with either ^{111}In or ^{90}Y. Nude mice bearing intra-abdominal lumps of a human colorectal carcinoma cell line (SW620) were used as a model for peritoneal carcinomatosis. A human monoclonal antibody IgMλ (CR4E8) reactive with human squamous-cell carcinoma was used as a control. **Results:** Indium-111-IgM and ^{90}Y-IgM immunoconjugates were compared in nude mice at 2, 24, 72, 120 and 144 hr after intraperitoneal administration. Both showed high specific tumor uptake. The tumor-effective half-lives of the immunoconjugates were 39 hr for indium and 46 hr for yttrium. Tumor-to-normal organ ratios were high and similar for both reagents. Only the femur uptake at later time points was relatively higher for the ^{90}Y-IgM than for ^{111}In-IgM. The tumor uptake of specific AC6C3-2B12 was about fourfold higher than the uptake of aspecific CR4E8 at 24 and 120 hr. **Conclusion:** The combination of ^{111}In- and ^{90}Y-labeled AC6C3-2B12 offers a new opportunity to develop safer and more effective methods for diagnosing and treating human patients with peritoneal carcinomatosis.

Key Words: indium-111; yttrium-90; human IgM; biodistribution; intraperitoneal administration

J Nucl Med 1996; 37:1545–1551

Received Sept. 8, 1995; revision accepted Dec. 13, 1995.
For correspondence or reprints contact: Syed M. Quadri, PhD, Department of Experimental Radiotherapy, Box 66, The University of Texas, M.D. Anderson Cancer Center, 1515 Holcombe Blvd., Houston, TX 77030.

A radiolabeled immunoglobulin therapy (RIT) strategy can be applied rationally and safely if results of a diagnostic radioimmunoconjugate are predictive for results of a therapeutic radioimmunoconjugate. First, patients receive an immunoconjugate reactive with tumor-associated antigens as a diagnostic reagent labeled with a gamma-emitting isotope. If immunoscintigraphy studies with a gamma camera show that the radioimmunoconjugate behaves satisfactorily in vivo, the same immunoconjugate can be administered again, now labeled with a beta-emitting isotope, for treatment. The diagnostic study with a gamma-emitting reagent can be performed in an outpatient setting because the total administered activity is low. Subsequent therapy with beta-emitting isotope can also be accomplished on an outpatient basis because most of the beta-emission energy is absorbed in vivo within a few millimeters of the radioimmunoconjugate.

Previous experience in preclinical and clinical RIT has shown that under the proper conditions, the administration of ^{111}In-labeled immunoconjugate before the introduction of the same immunoconjugate labeled with ^{90}Y can be useful in predicting tumor targeting and tumor dosimetry before therapy (*1–10*). The physical characteristics of ^{111}In and ^{90}Y are well-suited for the diagnosis and treatment of cancer, respectively. Both radiometals require a bifunctional chelating agent for stable binding to an immunoglobulin. The coordination chemistries of ^{90}Y and ^{111}In are similar but not identical; therefore, the combined use of indium- and yttrium-labeled immunoconjugates requires prior verification and correlation of their in vivo pharmacokinetic characteristics, such as chelation stability, tumor uptake and biodistribution.

Two problems have impeded the broader application of RIT in patients: low uptake of radioimmunoconjugate in tumors

(*11*) and anti-mouse antibody formation in vivo (*12–15*). A potential solution to the problem of low tumor uptake would be to place the radioimmunoconjugates in direct contact with the tumor. This could be accomplished by intraperitoneal (i.p.) instead of intravenous (i.v.) administration of a RIT reagent in patients with peritoneal carcinomatosis. This compartmental i.p. approach bypasses the endothelial barrier existing between an i.v. RIT reagent and tumor and allows for high, local concentrations of immunoconjugate and direct access to the tumor (*16,17*). Comparisons between i.v. and i.p. administration of IgM in nude mice with peritoneal tumor nodules have shown that the i.p. approach results in higher tumor uptake, lower blood activity, and better tumor-to-normal tissue ratios (*18*). The development of human monoclonal antibodies (MAbs) reactive with adenocarcinomas, including ovarian and colon cancers, is important because the administration of human MAbs does not induce the formation of clinically significant human anti-human antibodies (*13*) and would allow for repeated administrations while maintaining efficacy.

The majority of patients with ovarian cancer are diagnosed at a stage of disease when the malignancy has spread to the peritoneal cavity (*19,20*). Treatments for peritoneal metastatic tumors have included i.v. or i.p. chemotherapy, external beam radiotherapy and i.p. radiocolloids (*21–24*). Cure rates with these treatment modalities have been modest at best, and side effects are frequent. Ovarian cancer is often confined to the peritoneal cavity, which provides an excellent opportunity to test a potentially less toxic treatment approach, i.p. RIT (*20,25–27*). Clinical trials with i.p. RIT using ^{90}Y-labeled murine monoclonal HMFG1 IgG_1 have shown the feasibility of this approach and have demonstrated favorable tumor-to-normal tissue ratios and selective tumor uptake (*27–29*).

In this study, the biodistribution of human monoclonal IgM AC6C3-2B12 labeled with ^{111}In or ^{90}Y was analyzed in nude mice bearing abdominal tumor lumps of a human colorectal carcinoma cell line (SW620).

MATERIALS AND METHODS

Production and Analysis of Antibody

AC6C3-2B12 was developed previously by Freedman et al. (*30*). AC6C3-2B12 is a human monoclonal IgMλ and recognizes a 32-kDa determinant expressed on the cell surface of various malignancies including ovarian cancer, colon cancer, and some malignancies of neuroectodermal origin (*30*). Another human monoclonal IgMλ (CR4E8), also developed by Freedman et al., that reacts with squamous-cell carcinomas was used as a specificity control (*31*). This antibody recognizes an antigen present in human cervix cancer with squamous-cell histology. IgM antibodies were purified from cell culture supernatant as previously described (*18*). The specific binding of IgM and IgM-chelate conjugate was determined by a fluorescence-activated cell sorter (FACS) technique previously reported (*30*). The immunoreactivity of radiolabeled IgM conjugate was tested in a direct cell-binding assay under antigen excess conditions (*32*).

Cell Line and Animal Model

The SW620 cell line was obtained from Dr. Janet Price (The University of Texas M. D. Anderson Cancer Center). Cells were grown as a monolayer culture in RPMI medium containing 10% fetal calf serum in the presence of 5% CO_2 at 100% humidity and 37°C. Cells were harvested after incubation for 2 min with 0.05% trypsin at 37°C, washed once in RPMI and resuspended in a concentration of 8×10^6 cells in 0.2 ml RPMI media.

Six-week-old female nude mice nu/nu weighing 20–25 g were housed in filter-top cages in a closed, environment-controlled colony and given sterile food and water. Each mouse was ear-tagged for identification. The cell suspension (0.2 ml) was injected directly into their peritoneal cavities through the abdominal wall using a 25-gauge needle. The animals' health and growth of their tumors were monitored daily. Animal studies were conducted in compliance with the USDA and Animal Welfare Act. Animal protocols were approved by the Animal Care and Use Committee at the M.D. Anderson Cancer Center.

Immunoconjugate Preparation

A carbon-backbone-modified chelator, 2-aminobenzyl-3-methyl diethylenetriamine-pentaacetic acid (2B3M-DTPA) was prepared as previously described (*33*). The primary amine group of 2B3M-DTPA was converted into an isothiocyanato derivative (ITC-2B3M-DTPA) for protein conjugation. AC6C3-2B12 (9 mg, 1×10^{-5} mmol) was reacted with ITC-2B3M-DTPA (80 μg, 13×10^{-5} mmol) at a molar ratio of 1:13 in 2 ml of 0.2 *M* bicarbonate buffer, pH 8.4, at 4°C for 12 hr. Before radiolabeling, chelate-immunoconjugates were purified from unconjugated chelate molecules by Centricon-30 filtration. The average number of chelates conjugated to each IgM molecule was determined as previously described (*34*). The purity of the IgM-chelate conjugates was analyzed by size-exclusion, high-performance liquid chromatography (HPLC). A 10-μl sample of IgM-chelate solution was injected onto the size-exclusion HPLC column. The column was connected to an isocratic HPLC system. The sample was eluted at a flow rate of 1 ml/min, and the elution was monitored at a wavelength of 280 nm using an ultraviolet detector.

Radiolabeling of IgM Conjugates

Indium-111-chloride was obtained from DuPont NEN Products (Wilmington, DE). A 20-μl aliquot of $^{111}InCl_3$ (3.7 mCi) was equilibrated with 250 μl of 0.6 *M* sodium acetate buffer, pH 5.3, and 250 μl of 0.06 *M* sodium citrate buffer, pH 5.5. Two hundred and fifty microliters of immunoconjugate (6 mg/ml) in 0.1 *M* phosphate-buffered saline (PBS) was added to buffered indium, mixed well, and incubated at room temperature for 45 min. This labeling mixture was challenged with a 100-fold excess of free DTPA to sequester free isotope and remove weakly-labeled radioisotopes from the protein before column chromatography. The radiolabeled immunoconjugate was separated from low molecular weight compounds by gel filtration chromatography with a 1.5 × 20-cm Sephadex G50 gel column using 0.1 *M* PBS as an eluant.

Yttrium-90-chloride was obtained from Westinghouse (Richland, WA). A 5-μl aliquot of $^{90}YCl_3$ (6.5 mCi) in 0.1 *M* HCl was equilibrated with 200 μl 2.0 *M* acetate buffer, pH 6.0. An aliquot of 200 μl of immunoconjugate solution (6 mg/ml) in 0.1 *M* PBS was added to buffered ^{90}Y solution, mixed well and incubated at room temperature for 90 min. DTPA challenge and gel-filtration chromatography purification was similar to the procedure used in ^{111}In labeling, except that a 1.5 × 30-cm Sephadex G100 gel column was used.

The incorporation of radiometals to immunoconjugates was monitored by instant thin-layer chromatography (ITLC) and thin-layer chromatography (TLC) analyses after the incubation period (radiochemical yield), after DTPA challenge, and after column elution (final product). Radiolabeling efficiency, radiochemical yield, and specific activity of all the radioimmunoconjugates were determined. Samples were spotted on ITLC strips (silica-gel-impregnated glass fiber) and developed with 9% saline for both the ^{111}In- and ^{90}Y-labeled products. TLC analyses were performed similarly with 10% ammonium acetate/methanol (1:1) and NH_4OH/ethanol (1:4) as the developing solvent for indium- and yttrium-labeled immunoconjugates, respectively. Before the final product was administered, the labeled immunoconjugate solution

TABLE 1
Quality Control Analysis of IgM Conjugates

Analysis	Radioimmunoconjugate		
	^{111}In-IgM (AC6C3-2B12)	^{90}Y-IgM (AC6C3-2B12)	^{90}Y-IgM (CR4E8)
Average DTPA/IgM	4.0	4.0	4.0
Purity of immunoconjugate			
Size-exclusion HPLC	98%	98%	98%
Protein-bound radioactivity	98.3%	93.9%	96.5%
Specific activity	1.48 mCi/mg	3.25 mCi/mg	3.25 mCi/mg
Immunoreactivity	78%	61%	12%
Cell-binding assay FACS analysis	61%	61%	4.7%
Serum stability*	90.2%	94.2%	—
Activity injected per animal	15 μCi	28 μCi	28 μCi

*Protein-bound fraction after 48 hr incubation at 37°C in human serum.

was filtered through a sterile 0.2-μm Acrodisc syringe filter (Gelman Sciences, Inc., Ann Arbor, MI).

Radioimmunoconjugate Administration and Biodistribution

Seventeen days after tumor inoculation, nude mice with i.p. tumor lumps were selected for biodistribution. The nude mice bearing exclusively i.p. SW620 lumps were injected i.p. with either ^{111}In- or ^{90}Y-labeled AC6C3-2B12 conjugates. The syringe was weighed before and after injection to determine the exact amount of radioactivity administered.

For biodistribution studies, four mice were killed at each time point (2, 24, 72, 120, and 144 hr postinjection). Approximately 0.5 ml of blood was removed by cardiac puncture, weighed and prepared for radioactivity assay. Intraperitoneal tumor lumps and normal-tissue samples (whole organs in every case, except for the liver and small intestines) were removed, cleaned in saline, weighed, and assayed for radioactivity. Instruments were cleaned with 70% ethanol between organ samplings to reduce cross-contamination. A Cobra II gamma counter (Packard Instrument Co., Downers Grove, IL) was used to determine counts per minute per gram of sample. A standard of the injectate was counted simultaneously to correct data for the physical decay of the isotopes. The counting efficiencies were approximately 73.3% (150-500 keV window) for ^{111}In and 16.5% (50–1000 keV window) for ^{90}Y. The low counting efficiency for ^{90}Y is caused by the use of bremsstrahlung emissions for detection. Percent injected dose/gram was calculated for all samples.

Yttrium-labeled human CR4E8 (the control IgM) was administered i.p. into 8 mice for biodistribution studies at 24 and 120 hr postinjection.

Statistical Analysis

The biodistribution differences between ^{111}In-IgM and ^{90}Y-IgM were compared at different time points using the Wilcoxon rank sum test. The traditional $p < 0.05$ value was used to indicate statistical significance.

RESULTS

Quality Control Analysis

Table 1 shows the quality control analysis of immunoconjugates labeled with ^{111}In or ^{90}Y. Size-exclusion HPLC analysis indicated a purity of 98% IgM protein after protein purification. On average, four 2B3M-DTPA chelates were conjugated per IgM molecule. The radiochemical purity reflects the percentage of isotope bound to the chelate-immunoconjugate in the final product. The radiolabeling protocol provided high labeling efficiency and a final labeled product with more than 95% of the isotope bound to chelate-immunoconjugate. The immunoreactivity analysis showed 70–80% of radiolabeled IgM bound to viable SW620 tumor cells, whereas the (CR4E8) control demonstrated only 12% binding. FACS analysis of the reactivity of SW620 with AC6C3-2B12 conjugates showed 61% cell-surface reactivity versus only 4.7% with CR4E8 conjugates. The serum stability of the radioimmunoconjugates was tested by ITLC and TLC analyses after a 48-hr incubation in human serum at 37°C. Approximately 90% of ^{111}In and 94% of ^{90}Y labels remained bound to protein.

Biodistribution of AC6C3-2B12

The biodistribution data for ^{111}In- and ^{90}Y-labeled AC6C3-2B12 conjugates are shown in Figure 1. A small amount of radioactivity was found in the blood at 2 hr (0.5% ± 0.1% ID/g)

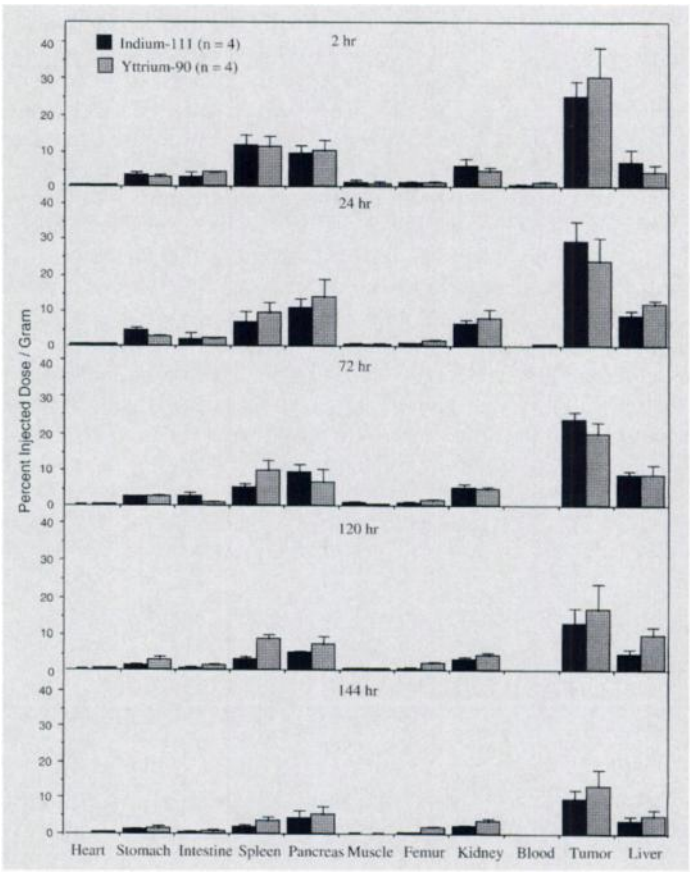

FIGURE 1. Biodistribution of ^{111}In- and ^{90}Y-labeled AC6C3-2B12 conjugates after i.p. administration to nude mice bearing intraperitoneal tumor lumps (SW620).

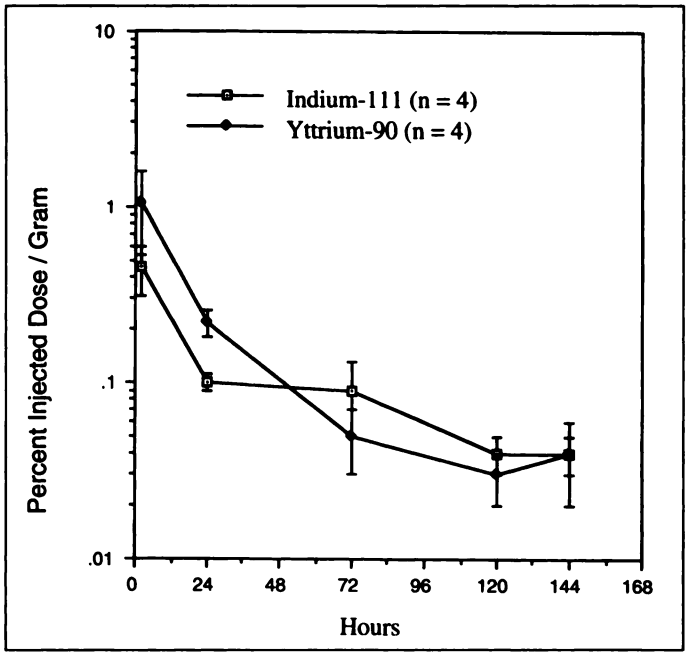

FIGURE 2. Blood clearance of ^{111}In- and ^{90}Y-labeled AC6C3-2B12 conjugates after i.p. administration to nude mice with intraperitoneal tumor lumps (SW620).

and subsequently decreased to 0.04% ± 0.02% ID/g at 144 hr. For both indium- and yttrium-labeled immunoconjugates, the biological half-lives of blood were biphasic with a high ratio between fast and slow elimination pathways (Fig. 2). This is probably due to the presence of low molecular weight radioactive components in blood with rapid urinary elimination. TLC studies of urine radioactivity in these mice confirmed a low-molecular-weight moiety similar to a DTPA metal complex. At all time points, the highest amount of radioactivity was found in the tumor with a maximum of 29.0% ± 5.8% ID/g for ^{111}In at 24 hr and 31.7% ± 8.6% ID/g for ^{90}Y at 2 hr. Moderately high radioactivity, less than 12% ID/g, was present in the pancreas, spleen, kidney and liver at early time points. Pancreas, kidney and liver uptakes showed a clearance pattern similar to that of tumor uptake. The effective half-lives of radioactivity in these organs is monophasic (Table 2). Activity in the spleen cleared more quickly, decreasing from 11.6% ± 3.0% ID/g at 2 hr to 6.7% ± 2.6% ID/g at 24 hr.

Significant similarities were found between ^{111}In- and ^{90}Y-labeled AC6C3-2B12 (Figs. 1 and 2; Table 3). The statistical analysis summary in Table 3 indicates that most organs at most time points have similar radioactivity levels for the two radiolabels. As an exception, gradually more ^{90}Y than ^{111}In is found

TABLE 2
Effective Half-Lives of Radioimmunoconjugates in Tumor-Bearing Nude Mice*

Organ	^{111}In-IgM (AC6C3-2B12) $t_{1/2}$ (hr)	^{90}Y-IgM (AC6C3-2B12) $t_{1/2}$ (hr)
Liver	40	39
Spleen	34	38
Pancreas	39	39
Tumor	39	46

*Data calculated from computer-fitted curves based on the mean uncorrected counts per minute per gram for 24, 72, 120 and 144 hr time points, four mice per time point per label.

TABLE 3
Statistical Analysis of ^{111}In and ^{90}Y Biodistribution Comparison*

Organ	Hr after injection 2	24	72	120	144
Spleen	ns	ns	0.025 (1.8)†	0.025 (2.9)	0.025 (2.2)
Pancreas	ns	ns	0.025 (0.6)	0.025 (1.6)	ns (1.7)
Kidney	ns	ns	ns	ns	0.025 (1.9)
Liver	0.025 (0.7)	ns	ns	0.025 (2.1)	ns
Femur	ns	0.05 (2.2)	ns (1.5)	0.025 (3.4)	0.025 (5.3)
Tumor	ns	ns	ns	ns	ns

*(n = 4). p values obtained by the Wilcoxon rank sum test are given (ns = not significant, $p > 0.05$).
† Ratio of ^{90}Y to ^{111}In mean biodistribution values.

in the femur. At 144 hr, five times more yttrium than indium is found in the femur. However, the ID/g for yttrium in the femur never exceeds 2%. Less than threefold differences are found between indium and yttrium for other organs. The assumption is that these differences are caused by contamination of normal organs of some animals with thin sheets of peritoneal carcinomatosis.

Tumor-to-Normal Organ Ratio

The ratio of radioactivity uptake in tumor versus in normal organs surrounding the peritoneal cavity and in muscle and femur is shown in Table 4. For both radioimmunoconjugates, the organ with the lowest tumor-to-normal organ ratio was the pancreas. Its ratio remained at 2 or 3 at all time points. This might have been caused by cross-reactivity of the immunoglobulin with pancreatic antigens of the mouse or by tumor growth in the proximity of pancreatic tissue. The tumor-to-blood ratio ranged from low values of 57 for indium and 29 for yttrium at 2 hr, to peak values of 317 and 559, respectively, at 120 hr. For other organs, tumor-to-normal organ ratios were stable over the 144-hr period. At later time points, the most significant difference between the two labels was the higher tumor-to-femur ratio for ^{90}Y (Tables 3 and 4).

Control IgM (CR4E8)

The biodistribution comparison of the ^{90}Y-labeled aspecific human monoclonal IgM CR4E8 control and the specific human monoclonal IgM AC6C3-2B12 is given for two time points in Figure 3 and Table 5. The uptake of CR4E8 in the tumor was 5.3% ± 2.0% and 3.6% ± 1.3% ID/g at 24 and 120 hr, respectively. The tumor uptake of ^{90}Y-labeled AC6C3-2B12 was high compared with the uptake of CR4E8, i.e., 4.5 and 4.6 times higher at 24 and 120 hr, respectively (Table 5). For some normal organs, the radioactivity retention of AC6C3-2B12 and CR4E8 varied, presumably because of the difference in reactivity of the two immunoglobulins. At 24 and 120 hr, the ratios between specific and aspecific radioimmunoconjugate uptakes were 1.9 and 0.9 for pancreas, 0.9 and 1.7 for spleen, 1.7 and 1.0 for kidney and 1.9 and 2.6 for liver, respectively.

DISCUSSION

The i.p. administration of a human monoclonal IgM that targets peritoneal tumors may provide a more effective, less toxic therapy for human patients suffering from peritoneal carcinomatosis. There is suggestive evidence to support this

TABLE 4
Tumor-to-Organ Ratios of Indium-111- and Yttrium-90-IgM in Nude Mice Bearing Peritoneal Tumor Lumps (SW620)

	Hr after i.p. administration									
	2		24		72		120		144	
Organ	^{111}In	^{90}Y	^{111}In	^{90}Y	^{111}In	^{90}Y	^{111}In	^{90}Y	^{111}In	^{90}Y
Stomach	8	12	7	9	9	9	10	7	10	9
Spleen	2	3	4	3	5	2	4	2	6	4
Pancreas	3	3	3	2	3	3	3	2	2	2
Kidney	4	7	5	3	5	4	4	4	5	4
Liver	4	8	4	2	3	2	3	2	3	3
Muscle	26	38	62	61	41	65	55	65	60	76
Femur	28	35	49	18	28	18	29	11	27	7

hypothesis. First, the problem of moving a large-size IgM radioimmunoconjugate (950,000 mol. wt.) through the blood vessel walls to the site of the tumor is eliminated by direct i.p. injection. Second, the residence of the IgM pentamer in the peritoneal cavity is prolonged in comparison to that of the smaller IgG molecules (e.g., IgG 150,000 mol. wt., *unpublished observations*), thus increasing the exposure of radioimmunoconjugate to the tumors and decreasing the radioactivity level in the blood. Third, human monoclonal antibodies directed toward a human cancer may avoid the problem of antibody induction and allow for repeated, "fractionated" use of the radioimmunoconjugate in human patients.

This animal study demonstrates specific targeting of human cancer cells and low normal-tissue uptake of a human IgM after i.p. administration. This compartmental approach is characterized by early (2 hr) uptake of the labeled immunoconjugate in the tumor, suggesting that the absence of an endothelial barrier indeed removes a major limitation to tumor uptake after i.v. administration (*18*). The effective clearance of tumor radioactivity is slow, i.e., approximately 40 hr. Selective retention may be related to strong IgM binding to tumor antigens. Some organs around the peritoneal cavity, e.g., pancreas, spleen, kidney, and liver, show moderate uptake. Part of this uptake might be caused by cross-reactivity of the immunoglobulin between normal mouse and human antigens, by filtration of large IgM molecules in the reticuloendothelial system or by the involvement of normal mouse organs in the peritoneal carcinomatosis process.

In other preclinical and clinical studies, blood radioactivity correlated positively with hematological toxicity (*10,35*). Bone marrow damage has been the first-line, dose-limiting normal tissue toxicity in most clinical RIT studies to date (*5*). Blood radioactivity remained very low after i.p. administration in this study, indicating that most of the radioimmunoconjugate remained in and around the peritoneal cavity. Therefore, bone marrow toxicity is not expected to be the dose-limiting normal tissue toxicity after i.p. radiolabeled IgM therapy. Further preclinical investigation is required to determine the radiotoxicity of ^{90}Y-labeled IgM to normal tissues in the peritoneal cavity. In mice, the i.p. RIT will provide almost homogenous whole liver, kidney, and intestinal irradiation because these organs are small and because of the long range of the ^{90}Y emissions. Studies using beagle dogs with anatomic dimensions closer to those of human patients will provide a more realistic model than nude mice studies (*35*). In addition, one of the organs with a moderate amount of radioactivity uptake in the mouse, i.e., the liver, has the same radiosensitivity to radiation in humans and dogs (*36*).

Like blood, other organs that do not surround the peritoneal cavity, such as thigh muscle, femur, and heart, showed little radioactivity uptake, again demonstrating that both radioimmunoconjugates remained well localized in the peritoneal cavity. The low level of radioactivity in the blood and the biphasic disappearance curve of radioactivity in the blood suggest that

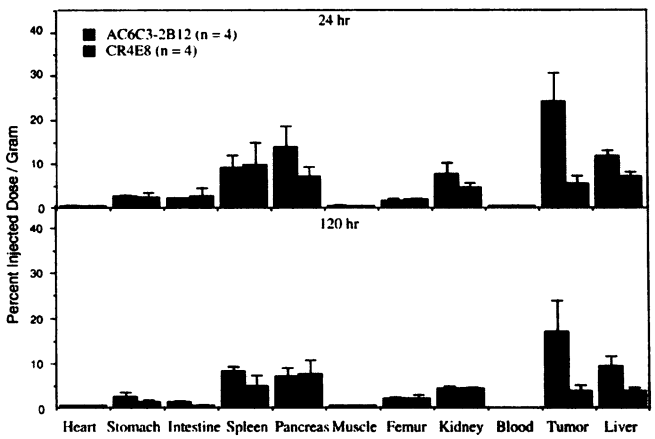

FIGURE 3. Comparative biodistribution of ^{90}Y-labeled AC6C3-2B12 (specific) and CR4E8 (aspecific control) conjugates at 24 and 120 hr after i.p. administration to nude mice bearing intraperitoneal tumor lumps (SW620).

TABLE 5
Ratio of Specific AC6C3-2B12 to Aspecific CR4E8 Uptake in Nude Mice Bearing Intraperitoneal Tumor Lumps (SW620)*

	Hr after i.p. administration	
Organ	24	120
Tumor	4.5	4.6
Liver	1.9	2.6
Spleen	0.7	1.7
Pancreas	1.9	0.9
Kidney	1.7	1.0
Stomach	1.1	1.9
Small intestine	0.8	2.9
Blood	1.0	0.7
Femur	1.1	0.7
Heart	1.6	0.9
Muscle	2.3	1.0

*AC6C3-2B12 is a human monoclonal IgM reactive with human adenocarcinoma including SW620. CR4E8 is a human monoclonal IgM reactive with an antigen present on human cervical cancer with squamous cell histology.

the small amount of radiolabeled moieties that escape the peritoneal cavity are mostly of low molecular weight. This may be caused by catabolism of the immunoglobulin or some trace amounts of chelated indium or yttrium. The dominant escape route from the peritoneal cavity for the intact IgM is by transdiaphragmatic lymph vessels and mediastinal lymph nodes (*18*).

Bone uptake was increased after catabolism of ^{90}Y-labeled i.p. IgM. This increased uptake was not noticed after i.v. IgM, indicating that the catabolism of IgM might be different in different compartments in the body (*18*). The total uptake in bone of ^{90}Y remained low. Therefore, bone marrow toxicity is not expected to be dose-limiting to the i.p. administration of ^{90}Y-labeled IgM conjugate. Bone marrow dosimetry can still be performed on the basis of ^{111}In-labeled IgM if the differences between ^{90}Y and ^{111}In documented in this study are taken into account.

The potential therapeutic advantages of i.p. RIT over i.p. colloidal ^{32}P, whole abdominal external beam irradiation and intraperitoneal chemotherapy are significant for tumor dose and normal tissue toxicity. Phosphorus-32 colloids have no specific tumor uptake and have a short residence in the peritoneal cavity in animal models (*37*). External beam radiotherapy to the abdomen cannot deliver the dose required to destroy abdominal masses (> 2 cm in diameter, i.e., > 60 Gy) without exceeding normal tissue tolerance levels (*38*). Normal kidney, liver, and small intestine can only tolerate doses up to 20, 30, and 40 Gy, respectively. Intraperitoneal administration of cisplatin in patients with malignant ascites results in approximately 50 times more platinum in ascites than in plasma (*39*). Cisplatin is not expected to concentrate in the peritoneal carcinomatosis nodules. In comparison, we found that the uptake of i.p. administered ^{111}In-labeled AC6C3-2B12 in the tumor lumps ranged from 60 to 290 times higher than radioimmunoconjugate uptake in the blood over a prolonged period of time.

RIT with indium- and yttrium-labeled conjugates can be applied in an outpatient setting, thus increasing patient comfort and decreasing costs. Initial clinical RIT studies are best performed in patients with measurable disease so that tumor targeting and tumor response can be documented. Treatment with ^{90}Y-labeled IgM can be withheld from patients who show no tumor targeting with ^{111}In-labeled IgM and are not expected to benefit from RIT. After optimization of i.p. RIT in patients with measurable disease, further studies in patients with minimal disease can be conducted more safely and effectively.

CONCLUSION

Radiolabeled IgM conjugates appear to rapidly target intraperitoneal tumor lumps after i.p. administration, with most of the radioactivity being retained in the peritoneal cavity. These results indicate substantial similarities in the biodistribution of immunoconjugates labeled with ^{111}In or ^{90}Y in nude mice using the i.p. approach. Moreover, the high tumor-to-normal tissue ratios support the clinical development of IgM radioimmunoconjugates for i.p. treatment of patients with peritoneal carcinomatosis.

ACKNOWLEDGMENTS

This project was supported by National Institutes of Health grants CA 43791, CA 51161 and CA 16672.

REFERENCES

1. Order SE, Klein JL, Leichner PK, Frincke J, Lollo C, Carlo DJ. 90-yttrium antiferritin. a new therapeutic radiolabeled antibody. *Int J Radiat Oncol Biol Phys* 1986;12:277–281.
2. Leichner PK, Yang N-C, Frenkel TL, et al. Dosimetry and treatment planning for ^{90}Y-labeled antiferritin in hepatoma. *Int J Radiat Oncol Biol Phys* 1988;14:1033–1042.
3. Goldenberg DM. New developments in monoclonal antibodies for cancer detection and therapy. *Cancer J Clin* 1994;44:43–63.
4. Abdel-Nabi H, Doerr RJ. Clinical applications of indium-111-labeled monoclonal antibody imaging in colorectal cancer patients. *Semin Nucl Med* 1993;23:99–113.
5. Vriesendorp HM, Quadri SM, Williams JP. Radioimmunotherapy. In: Armitage JO, Antman K, eds. *High dose cancer therapy*. Philadelphia: Williams & Wilkins; 1992:84–123.
6. Leichner PK, Koral KF, Jaszczak RJ, Green AJ, Chen GT, Roeske JC. An overview of imaging techniques and physical aspects of treatment planning in radioimmunotherapy. *Med Phys* 1993;20:569–577.
7. Sharkey RM, Kaltovich FA, Shih LB, Fand I, Govelitz G, Goldenberg DM. Radioimmunotherapy of human colonic cancer xenografts with ^{90}Y-labeled monoclonal antibodies to carcinoembryonic antigen. *Cancer Res* 1988;48:3270–3275.
8. Vriesendorp HM, Herpst JM, Germack MA, et al. Phase I-II studies of yttrium-labeled antiferritin treatment for end stage Hodgkin's disease, including radiation therapy oncology group 87-01. *J Clin Oncol* 1991;9:918–928.
9. Hnatowich DJ, Chinol M, Siebecker DA, et al. Patient biodistribution of intraperitoneally administered yttrium-90-labeled antibody. *J Nucl Med* 1988;29:1428–1434.
10. Herpst JM, Klein JL, Leichner PR, Quadri SM, Vriesendorp HM. Survival of patients with treatment resistant Hodgkin's disease after yttrium-90-antiferritin. *J Clin Oncol* 1995;13:2394–2400.
11. Dykes PW, Gradwell AR, Chapman CE, Vaughan ATM. Radioimmunotherapy of cancer: clinical studies and limiting factors. *Cancer Treat Rev* 1987;14:87–106.
12. Schroff RW, Foon KA, Beatty SM, Oldham RK, Morgan AC. Human anti-murine immunoglobulin response in patients receiving monoclonal antibody therapy. *Cancer Res* 1985;45:879–885.
13. DeJager R, Abdel-Nabi H, Serafini A, Pecking A, Klein JL, Hanna MG Jr. Current status of cancer immunodetection with radiolabeled human monoclonal antibodies. *Semin Nucl Med* 1993;23:165–179.
14. Sands H, Jones PL. Methods for the study of the metabolism of radiolabeled monoclonal antibodies by liver and tumor. *J Nucl Med* 1987;28:390–398.
15. Reynolds JC, DelVecchio S, Sakahara H, et al. Antimurine antibody response to mouse monoclonal antibodies: clinical findings and implication. *Int J Radiat Appl Inst (B)* 1989;16:121–125.
16. Rowlinson G, Snook D, Busza A, Epenetos AA. Antibody-guided localization of intraperitoneal tumors following intraperitoneal or intravenous antibody administration. *Cancer Res* 1987;47:6528–6531.
17. Larson SM, Carrasquillo JA, Colcher DC, et al. Estimates of radiation absorbed dose for intraperitoneally administered iodine-131 radiolabeled B72.3 monoclonal antibody in patients with peritoneal carcinomatosis. *J Nucl Med* 1991;32:1661–1667.
18. Quadri SM, Malik AB, Tang X-Z, Patina R, Freedman RS, Vriesendorp HM. Preclinical analysis of intraperitoneal administration of indium-111 labeled human tumor reactive monoclonal IgM AC6C3-2B12. *Cancer Res* 1995;55:5736S–5742S.
19. Greenberg PAC, Kudelka AP, Kavanagh JJ. Ovarian cancer. In: Pazdur R, eds. *Medical oncology: a comprehensive review*. Huntington, NY: PRR, Inc.; 1993;233–242.
20. Rubin SC. Monoclonal antibodies in the management of ovarian cancer: a clinical perspective. *Cancer* 1993;71(suppl):1602–1612.
21. Schray MF, Martinez A, Howes AE. Advanced epithelial cancer: salvage whole abdominal radiation for patients with recurrent or persistent disease after combination therapy. *J Clin Oncol* 1988;6:1433–1439.
22. Reichman B, Markman M, Hakes T. Intraperitoneal cisplatin and etoposide in the treatment of refractory/recurrent ovarian carcinoma. *J Clin Oncol* 1989;7:1327–1332.
23. Julian CG, Inalsingh CH, Burnett LS. Radioactive phosphorus and external radiation as an adjuvant to surgery for ovarian cancer. *Obstet Gynecol* 1978;52:155–160.
24. Rosenshein NB, Leichner PK, Vogelsang GR. Radiocolloids in the treatment of ovarian cancer. *Obstet Gynecol* 1979;34:708–720.
25. Crippa F. Radioimmunotherapy of ovarian cancer. *Int J Biol Markers* 1993;8:187–191.
26. Schneider-Gadicke E, Humm JL, Lau CC, Macklis RM, Bastert G, Knapp RC. Analysis of cytotoxicity of ^{131}I-labeled OC125 F(ab')^2 on human epithelial ovarian cancer cell lines. *Radiother Oncol* 1992;23:150–159.
27. Stewart JSW, Hird V, Dhokia B, et al. Intraperitoneal yttrium-90-labeled monoclonal antibody in ovarian cancer. *J Clin Oncol* 1990;8:1941–1950.
28. Hird V, Maraveyas A, Snook D, et al. Adjuvant therapy of ovarian cancer with radioactive monoclonal antibody. *Br J Cancer* 1993;68:403–406.
29. Maraveyas A, Snook D, Hird V, et al. Pharmacokinetics and toxicity of an yttrium-90-CITC-DTPA-HMFG1 radioimmunoconjugate for intraperitoneal radioimmunotherapy of ovarian cancer. *Cancer* 1994;73:1067–1075.
30. Freedman RS, Ioannides CG, Tomasovic B, et al. Development of a cell surface reacting human monoclonal antibody recognizing ovarian and certain other malignancies. *Hybridoma* 1991;10:21–33.
31. Chen P-F, Freedman RS, Chernajovsky Y, Platsoucas CD. Amplification of immunoglobulin transcripts by the non-palindromic adaptor polymerase chain reaction (NPA-PCR): nucleotide sequence analysis of two human monoclonal antibodies recognizing two cell surface antigens expressed in ovarian, cervix, breast, colon, and other carcinomas. *Hum Antibodies Hybridomas* 1994;5:131–142.
32. Lindmo T, Boven E, Cuttitta F, Fedorka J, Bunn PA Jr. Determination of the immunoreactive fraction of radiolabeled monoclonal antibodies by linear extrapolation to binding at infinite antigens excess. *J Immunol Methods* 1984;72:77–89.
33. Quadri SM, Mohammadpour H. A convenient synthesis of 2-p-aminobenzyl-3-methyl and 2-p-aminobenzyl-3-benzyl derivatives of diethylenetriaminepentaacetic acid (DTPA): carbon backbone modified bifunctional chelating agents. *Bio Med Chem Lett* 1992;2:1661–1664.
34. Quadri SM, Vriesendorp HM, Leichner PR, Williams JR. Evaluation of indium-111-

and yttrium-90-labeled linker-immunoconjugates in nude mice and dogs. *J Nucl Med* 1993;34:938–945.
35. Quadri SM, Shao Y, Blum JE, Leichner PK, Williams JR, Vriesendorp HM. Preclinical evaluation of intravenously administered ^{111}In- and ^{90}Y-labeled B72.3 immu noconjugate (GYK-DTPA) in beagle dogs. *Nucl Med Biol* 1993;20:559–570.
36. Wang S, Quadri SM, Tang X-Z, et al. Liver toxicity induced by combined external beam irradiation and radioimmunoglobulin therapy. *Radiat Res* 1995;141:292–302.
37. Leichner PK, Rosenshein NB, Leibel SA, Order SE. Distribution and tissue dose of intraperitoneally-administered radioactive chromic phosphate (^{32}P) in New Zealand white rabbits. *Radiology* 1980;134:729–734.
38. Mychalczak BR, Fuks Z. The role of radiotherapy in the management of epithelial ovarian cancer. In: Markman M, Hoskins WJ, eds. *Cancer of ovary*. New York, NY: Raven Press; 1993;229–241.
39. Casper ES, Kelsen DP, Alcock NW, Lewis Jr. JL. Intraperitoneal cisplatin in patients with malignant ascites: pharmacokinetics evaluation and comparison with i.v. route. *Cancer Treat Rep* 1983;67:235–238.

Uptake of Technetium-99m-Tetrofosmin, Technetium-99m-MIBI and Thallium-201 in Tumor Cell Lines

Ali S. Arbab, Kiyoshi Koizumi, Keiji Toyama and Tsutomu Araki
Department of Radiology, Yamanashi Medical University, Tamaho-cho, Nakakoma-gun, Yamanashi-ken, Japan

We investigated the kinetics, cellular uptake and intracellular distribution of ^{99m}Tc-tetrofosmin in tumor cell lines and compared them with those of ^{99m}Tc-MIBI and ^{201}Tl. **Methods:** At specific intervals after incubation with radiotracers, cellular uptake was determined. Cells were also treated with nigericin, carbonyl cyanide m-chlorophenylhydrazone (CCCP) and ouabain to determine their effects on the uptake of the tracers. **Results:** Each tracer showed similar uptake kinetics in both cell lines, and a steady-state was maintained for at least 4 hr. Nigericin stimulated the uptake of both ^{99m}Tc-tetrofosmin and ^{99m}Tc-MIBI in HBL-2 cells, although it inhibited their uptake in SW-13 cells. Nigericin also inhibited 90% of ^{201}Tl uptake in both cell lines. Addition of CCCP caused 73%–97% release of accumulated ^{99m}Tc-MIBI from both cell lines with or without nigericin pretreatment, indicating that most of the accumulated ^{99m}Tc-MIBI was related to mitochondria. The effect of CCCP on accumulated ^{99m}Tc-tetrofosmin was less marked than that on ^{99m}Tc-MIBI in both cell lines, indicating that only a part of accumulated ^{99m}Tc-tetrofosmin, was related to mitochondria. Ouabain preincubation inhibited 74%–77% and 51%–53% of ^{201}Tl uptake in HBL-2 and SW-13 cells, respectively, as well as inhibited 22%–31% uptake of ^{99m}Tc-tetrofosmin in both HBL-2 and SW-13 cells. Uptake by the dead cells of either cell line was negligible for each tracer. **Conclusion:** Technetium-99m-tetrofosmin uptake depends on both cell membrane and mitochondrial potentials. Only a small fraction of ^{99m}Tc-tetrofosmin accumulates inside the mitochondria, while most ^{99m}Tc-MIBI accumulates inside the mitochondria. Thallium-201 uptake is partly independent of the Na^+, K^+ pump.

Key Words: tumor cell lines; technetium-99m-tetrofosmin; technetium-99m-MIBI; thallium-201; mitochondrial and cell membrane potentials

J Nucl Med 1996; 37:1551–1556

Thallium-201 chloride and technetium-99m-hexakis-isobutyl-isonitrile (^{99m}Tc-MIBI) are widely used as myocardial perfusion agents (*1–4*). Both agents have also shown potential utility in the detection of various tumors (*5–8*). However, the uptake mechanisms of these agents differ. The uptake of ^{201}Tl to myocardial and tumor cells is related to cell membrane potential and Na^+K^+ ATPase activity (*9–12*). On the other hand, that of ^{99m}Tc-MIBI to these cells is also related to cell membrane potential, although passage through this membrane involves passive diffusion (*13–15*). Furthermore, the behaviors of these agents inside the cells also differ. Technetium-99m-MIBI is localized mostly inside mitochondria due to negative mitochondrial membrane potential, whereas ^{201}Tl remains in the cytosolic compartment (*9–16*). Technetium-99m-ethylene-bis[bis(2-ethoxyethyl) phosphin] (^{99m}Tc-tetrofosmin), a newly developed compound of the diphosphin group, like ^{201}Tl and MIBI, is currently used as a myocardial perfusion agent (*17,18*) and may be utilized to detect various tumors. It is a monovalent lipophilic cation that rapidly enters the myocardial cells due to its lipophilic properties (*17,19*), although this property alone may not be the sole determinant.

The purposes of this study were to evaluate the uptake kinetics of ^{99m}Tc-tetrofosmin in tumor cell lines and to compare them with those of ^{99m}Tc-MIBI and ^{201}Tl. For this purpose, three chemical agents were used: nigericin, an ionophore that increases the mitochondrial membrane potential and disrupts the cell membrane potential (*20,21*); carbonyl cyanide m-chlorophenylhydrazone (CCCP), an uncoupler of oxidative phosphorylation that depolarizes the mitochondrial membrane potential (*22*); and ouabain, a cell membrane Na^+, K^+ ATPase inhibitor (*23*).

MATERIAL AND METHODS

Cell Lines

The Epstein-Barr virus-negative lymphoma B-cell line HBL-2 (*24*) was cultured in RPMI 1640 (contained in m*M*, $Ca(NO_3)_2$, 0.42; $MgSO_4$, 0.4; KCl, 5.36; $NaHCO_3$, 11.9; NaCl, 102.67; Na_2HPO_4, 5.36) supplemented with heat-inactivated 20% fetal bovine serum (FBS) and antibiotics (penicillin 10 IU/ml and streptomycin 50 μg/ml). Cells were cultured as suspensions in 225 cm^2 tissue culture flask in the growth medium at 37°C in a humidified 5% CO_2/95% air atmosphere. After priming for 1 wk with addition of new medium on alternate days, the cells were harvested by centrifugation at 1000 rpm for 1–2 min and then washed with fresh FBS-free medium. The cells were resuspended at a concentration of 1×10^6/ml in FBS-free medium, transferred to plastic tubes and kept at 37°C for at least 1 hr for equilibration. All tubes were pretreated with 0.5% bovine serum albumin (BSA) to minimize adhesion of the tracers to the surface of the tubes.

The small-cell carcinoma of the adrenal cortex cell line, SW-13 (*25*), was obtained commercially. The cells were cultured to

Received Oct. 13, 1995; revision accepted Mar. 6, 1996.
For correspondence or reprints contact: Ali Syed Arbab, MBBS, Department of Radiology, Yamanashi Medical University, Tamaho-cho, Nakakoma-gun, Yamanashi-ken, 409-38, Japan.